



Fluoride ions in groundwater of the Turkana County, Kenya, East Africa

Piotr Rusiniak¹ · Klaudia Sekuła¹ · Ondra Sracek² · Piotr Stopa¹

Received: 18 January 2021 / Revised: 11 May 2021 / Accepted: 27 May 2021 / Published online: 9 June 2021
© The Author(s) 2021

Abstract Groundwater samples were evaluated throughout Turkana County (Kenya, East Africa) while looking for drinking water sources. Some samples showed high concentrations of fluoride with values in the range of 0.15–5.87 mg/L. Almost 50% of the samples exceeded the WHO and Kenyan potable water standard guideline value of 1.5 mg/L for drinking water quality. The hydrogeochemical studies revealed that the dominant cation in water is Na⁺ and the dominant anion is HCO₃⁻ resulting in Na-HCO₃ type of groundwater, followed by Ca/Mg-HCO₃ or Na-SO₄ and Na-Cl in a few cases. Speciation modelling revealed that the groundwater is undersaturated with respect to gypsum and anhydrite, mostly undersaturated with respect to fluorite (6 samples are at equilibrium), and supersaturated or at equilibrium with respect to calcite (CaCO₃). Precipitation of calcite favours the dissolution of F-rich minerals in the alkaline medium. Simultaneously, groundwater is enriched with sodium and bicarbonate, probably as a result of chemical weathering of Na-feldspar. Investigated groundwater can be presumably used for drinking purposes from 17 wells, but a detailed investigation of other trace element concentrations is necessary.

Keywords Africa · Kenya · Fluoride · Groundwater · Drinking water · Speciation calculation

✉ Klaudia Sekuła
klaudia.sekula@agh.edu.pl

¹ Department of Hydrogeology and Engineering Geology, Faculty of Geology, Geophysics and Environmental Protection, AGH University of Science and Technology, Mickiewicza 30 Av, 30-059 Kraków, Poland

² Department of Geology, Faculty of Science, Palacky University Olomouc, 17. listopadu 12, 771 46 Olomouc, Czech Republic

1 Introduction

Fluorine (F) belongs to the halogen group (17th group in the periodic table), its prevalence in the Earth's crust reaches 0.06%–0.09% and classifies it at the 13th place in terms of occurrence among other elements (Singh et al. 2018). It is one of the important microelements for the human organism, thus its deficiency and also excess are adverse for human health. The range between desired (0.05–0.07 mg/kg body weight) and toxic dose (5 mg/kg body weight) for fluoride are quite narrow (Fordyce 2011; Ullah et al. 2017). The recommended concentration of fluoride ions in drinking water should not exceed 0.7 mg/L. The reported cases of fluoride poisoning mainly concerned toothpaste, mouth rinses, and supplements (Ullah et al. 2017). In the case of fluorine deficiency, the tooth enamel may not be protected against the sugar acids what can lead to tooth decay (Hsu et al. 2018; Singh et al. 2018). Long exposure to the high concentration of fluorine, above the guideline value (GV = 1.5 mg/L) recommended by the World Health Organization (2017), can lead to the dental (0.9–1.2 mg/L of fluorides supplied with drinking water and dependent on other exposure sources) or skeletal fluorosis (3–6 mg/L of F⁻ in drinking water). Fluoride ions in the human organism can co-precipitate with calcium ions as insoluble CaF₂ (fluorite) in the human body leading to hypocalcaemia (Pettifor et al. 1989; Fordyce 2011; Khairnar et al. 2015; Singh et al. 2018).

In water, it occurs predominantly as fluoride ion (F⁻), and its main source is minerals containing fluorine i.e., fluorite (CaF₂), cryolite (Na₃AlF₆), fluorapatite [Ca₅(-PO₄)₃F], and rock phosphate. These minerals are widely used in the glass industry (Deng et al. 2018), as an ingredient of insecticides (Podder et al. 2012), as well as in the future they could be used in biomedicine as bioimaging

agent (Milojkov et al. 2020). In the Earth's crust under high-temperature conditions, fluorine is more mobile (Ali et al. 2018). The process controlling the presence of fluorine in the environment is chemical weathering of minerals containing this element (natural origin) and anthropogenic activities i.e., application of phosphate fertilizers, dust fall in phosphate industrial area, and fluorine released from coal-burning (Pauwels et al. 2015; Dehbandi et al. 2017; Hong et al. 2018; Singh et al. 2018; Fuge 2019; Wang et al. 2019). In groundwater, the occurrence of fluorine is often linked to the volcanic rocks in crystalline basement aquifers (Ozsvath 2006). It can co-occur with arsenic (Alarcón-Herrera 2013; Alarcón-Herrera et al. 2020), and its concentration is controlled by alkalinity, and concentrations of calcium and bicarbonate (Saxena and Ahmed 2001; Ali et al. 2016, 2018). The main mineral source controlling aqueous fluoride geochemistry is the solubility of fluorite (Apambire et al. 1997; Edmunds and Smedley 2004). Moreover, much research indicated a negative correlation between Ca and F ions concentration. Furthermore, in waters with a low concentration of calcium ions, there is a strong positive correlation between sodium and fluorine ions. The high concentration of sodium ions increases the solubility of fluorite through the base exchange (Apambire et al. 1997).

The concentration of fluoride can be also sometimes connected with the depth of the borehole. In research published by Nair et al. (1984), a general tendency shows the positive trend between F^- concentration and depth in Kenya—the deeper the fluoride concentrations increase and are in the range of 1–5 mg/L. Guo et al. (2012) presented that the depth of the wells (up to 30 m) has no impact on the fluoride amount (0.3–2.57 mg/L) found in the Shihai (Inner Mongolia) groundwater. As well, Ali et al. (2018, 2019b) showed that the variability in fluoride concentration in Western Haryana (up to 19 mg/L), Sindh, and Punjab in Pakistan (0.1–3.9 mg/L) can be explained itself in the depth of the well with a negative correlation of -0.2 . On the other hand, Abdurahman and Zewdie (2018) presented the inversed relationship between F^- concentration (0.65–4.10 mg/L) and borehole depth (25–250 m).

Fluorine is one of the causes of natural groundwater pollution around the world i.e. in Sweden (Berger et al. 2016a, b), Brazil (Martins et al. 2018), India (Reddy et al. 2010; Mondal et al. 2014; Pauwels et al. 2015; Kumar et al. 2017, 2018; Raju 2017; Raj and Shaji 2017; Ali et al. 2018, 2019a; Gupta and Misra 2018; Laxmankumar et al. 2019; Kanagaraj and Elango 2019; Yadav et al. 2019a, b), Ghana (Craig et al. 2018; Zango et al. 2019), China (Hu et al. 2013; Zhang et al. 2017; Wu et al. 2018; Su et al. 2019), Pakistan (Rafique et al. 2015; Rashid et al. 2018; Ali et al. 2019b), Iran (Dehbandi et al. 2018; Enalou et al.

2018; Naderi et al. 2020), South Korea (Chae et al. 2007). In poor and developing countries, where there is a hardship with access to pure drinking water and the problem of fluorine groundwater pollution has also been encountered, e.g., in Nigeria (Emenike et al. 2018), Namibia (Sracek et al. 2015; Abiye et al. 2018;), Kenya (Gaciri and Davies 1993; Zevenbergen et al. 1996; Olaka et al. 2016), Ethiopia (Tekle-Haimanot et al. 2006; Rango et al. 2010, 2012, 2014, 2017; Kravchenko et al. 2014; Colombani et al. 2018), and Malawi (Msonda et al. 2007). To summarise, the general mechanism controlling the high concentration of F^- ions in groundwater has geogenic sources that are: long residence-time favouring water–rock interaction processes, evaporation, hydrogeochemical type changes during water flow (from $Ca-HCO_3$ to $Na-HCO_3$), weathering or dissolution of F-bearing minerals, geological setting i.e., presence of crystalline basement rocks within the wells or salt-rich geological formations, sorption and ion-exchange processes. The chemical composition of groundwater especially characterised by high concentrations of HCO_3^- and Na^+ and alkaline pH play the most primary role for fluoride release to the groundwater. Other factors, usually negligible, that affect the fluoride concentrations are anthropogenic i.e., agricultural activities (groundwater is enriched in F^- ions due to the leaching from fertilizers) or mining activity.

This work is focused on the prevalence of fluoride in groundwater from Turkana County, Kenya. In the case of the Kenyan groundwater, the major considerable source of its F-enrichment is a geogenic source and the processes responsible for that phenomena are discussed in this paper. The research is based on the archive's data obtained during looking for water that can serve as a source of drinking water for local communities. The objective is to identify wells with high fluoride concentrations and to determine processes responsible for the fluoride groundwater enrichment.

2 Local geology, material, and methods

2.1 Study area

Turkana is the largest county situated in the north-western part of Kenya. It covers 77,000 km² and constitutes about 43% of the total area of the Rift Valley Province in Kenya. This county includes the endorheic and alkaline (pH = 9.2) Turkana Lake (Fig. 1a) which forms a natural eastern boundary of this region. Turkana is split into 6 districts: Turkana North, Turkana West, Turkana Central, Loima, Turkana East and Turkana South. The study area has semiarid climate conditions based on Köppen classification (Fig. 1b, c). The average annual precipitation and

Fluoride ions in groundwater of the Turkana County, Kenya, East Africa

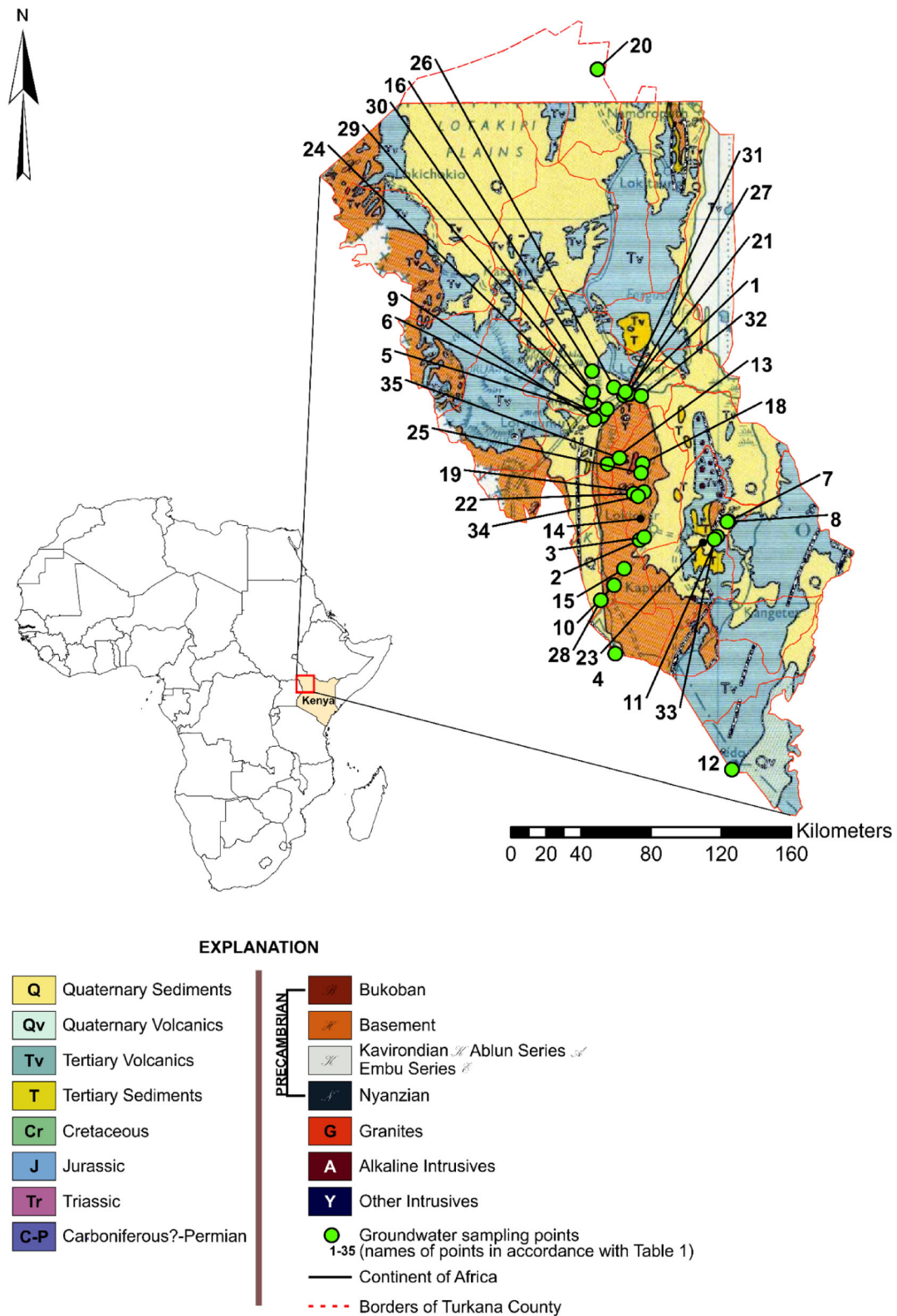


Fig. 1 Geology of Turkana County (Chief Geologist Mines and Geological Department 1962) and sampling points

temperature in the area are 210 mm and 29 °C, respectively. It is the poorest region in Kenya with frequent drought and famine problems. One of the major problems besides famines that people face out are droughts that occur every 2–4 years. It implies the water sources dry out, the number of sites with available water decreases, and the epidemics of water-borne diseases among people and animals break out (Oduor et al. 2012). In East Africa, during droughts, the recharge of the groundwater aquifers from the rainfall can be reduced even by 70% compared to the wet season, therefore the fluctuations in the groundwater table and changes in water quality are highly possible (Ferrer et al. 2019; Ochungo et al. 2020).

2.2 Geology

The geological setting of the study area is lithologically and tectonically variable. The oldest formations that can be observed in this area are metamorphized rocks of the Precambrian crystalline basement (Walsh and Dodson 1969). After deposition and deformation of the crystalline basement rocks, there was a stratigraphic gap. Precambrian rocks are covered with unconformable Cretaceous calcareous sedimentary rocks the so-called Turkana Grits, Paleogene-Neogene sedimentary, volcanic sediments, as well as the Quaternary sediments.

It is believed that the crystalline basement was formed from the sequence of the metamorphized sediments, volcanic rocks, and mafic and ultramafic intrusions. These sediments during orogenesis undergone successive compression, regional metamorphism, and injection of granites. As a result, there are gneisses, granulites, migmatites, quartzites and, marbles (Walsh and Dodson 1969). The crystalline basement rocks are observed in most of the geological profiles of the wells studied in this work. There are represented by gneisses with different mineral composition.

The Turkana Grits were firstly dated to the Jurassic age, but subsequent studies suggested periods from Cretaceous to Miocene (Dodson 1971). In studies from the 1960s, including the geological map presented in this work (Fig. 2), Miocene dating was adopted (Chief Geologist Mines and Geological Department 1962). Nowadays, due to the discoveries of dinosaur fossils (Handford 1987), they are now recognized as the Upper Cretaceous deposits. In the vast majority of the study area, the Turkana Grits occur as the calcareous, granular sandstones. These sediments occur in the north–west from the Tertiary volcanites (Tv)—on a map marked as Tertiary sediments (T), (Fig. 1).

The Tertiary series of volcanic rocks cover the upper Cretaceous sediments. They form the chain of hills running from the north to south in the eastern part of the study area

and on the north from Lodwar city. They are represented by fine crystalline basalts.

The Tertiary sediments include sandstones and shales of fluvial and limnic origin and are dated from the Paleogene to the middle Miocene. They fill the Paleogene Lokichar Basin covering the central and south–eastern part of the area, of the N–S orientation, 60 km long and 30 km wide (Tiercelin et al. 2004).

2.3 Hydrogeology

From the hydrogeological point of view, five-rock formations are essential for water supply in the Turkana Lake area. In the well profiles, there are alluvial sediments, Turkana Grits, and crystalline basement rocks. Others rocks are olivine basalts and phonolites linked to the Tertiary volcanic activity.

Crystalline basement rocks are characterised by a simple weathering profile. Along with the depth, the degree of weathering profile decreases to unweathered and low permeability rock. Groundwater, if found, usually occurs in the weathering zone close to its base, in local fissure systems and sediments above the basement rock. A good indicator of the likely occurrence of groundwater is the presence of a deep weathering zone and low clay content (Turkana Drilling Consortium 2008).

Lava's flow such as basalts and phonolites very rarely have significant primary porosity. Water usually can be found in the fissure zones, crevices and pyroclastic layers at the contact of different lava flows within the same lithology and so-called Old Land Surfaces. The thickness of such water-bearing horizons is generally limited to few metres (Turkana Drilling Consortium 2010).

The floodplains of the permanent and seasonal rivers are perspective areas for groundwater exploration. Often dried riverbeds are covered with water-bearing sandy alluvium. For Turkana nomads, shallow dug wells in the riverbeds are the most important, basic source of water. The Lokichar Basin located in the central and south–eastern part of the study area is often characterised as having a low potential for finding groundwater, especially with the growing distance from riverbeds (Turkana Drilling Consortium 2008).

3 Source of data

This study is based on the archival results of physico-chemical analyses performed for 35 points scattered throughout Turkana County from which groundwater was collected in the years 2004–2016. The water-bearing rocks were variable and included volcanic, sedimentary, and metamorphic rocks. The depth of the wells was from 17 to 80 m below surface level and two water horizons were

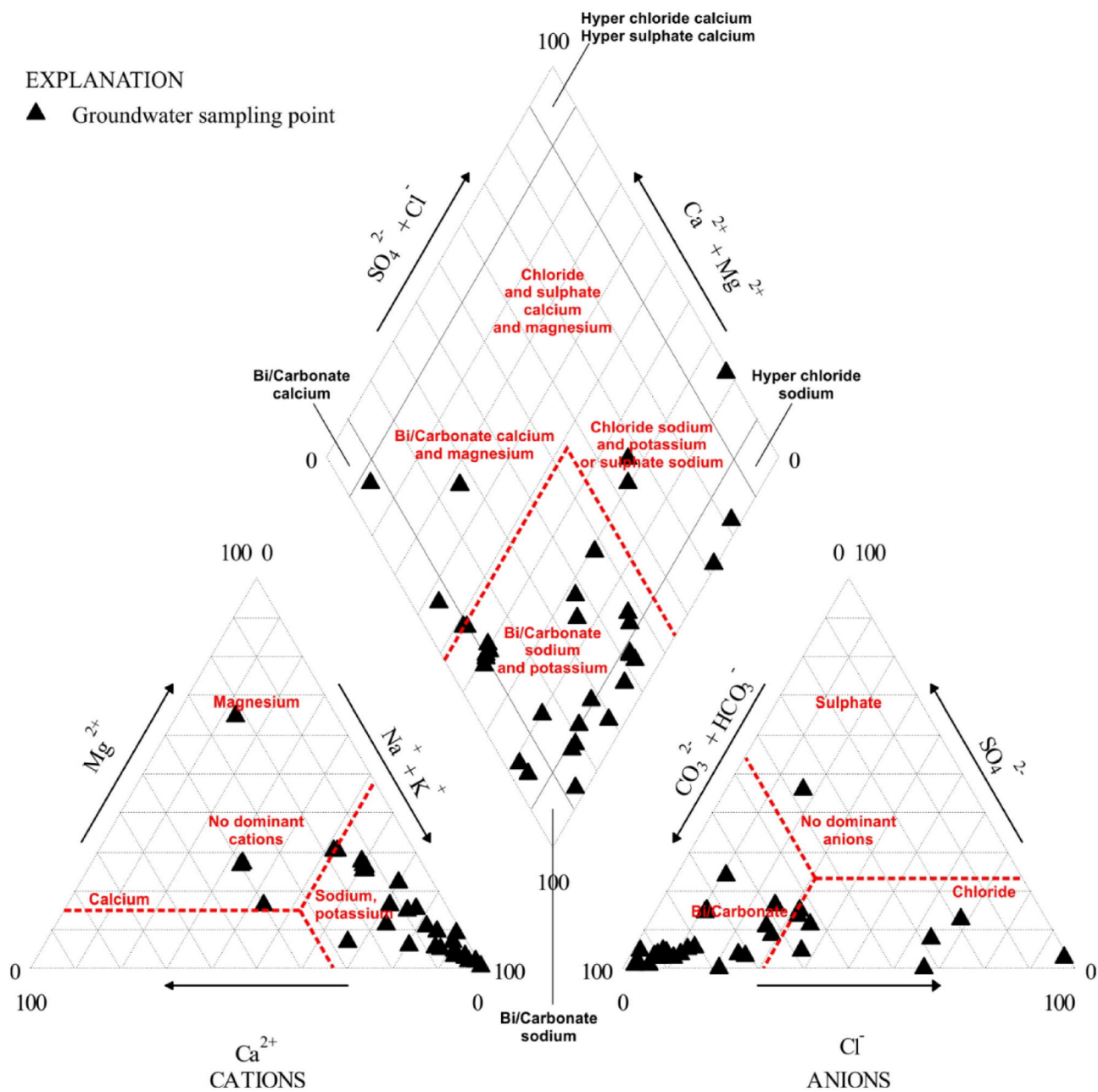


Fig. 2 Hydrogeochemical characteristics of groundwater using the Piper Diagram

recognized. The data used for the research purposes are archived and they were accessed from the Government Chemist’s Department of the Republic of Kenya (<https://www.govchemists.go.ke/>). The reports of the chemical analyses did not include the methods of analysis therefore the results of chemical analyses were checked by calculation of the charge balance error. All information about wells including the name of the sampling point, coordinates, year, and the results of chemical analysis are given in Table 1.

4 Results

4.1 Water chemistry

4.1.1 Hydrogeochemical facies

The hydrogeochemical characteristics including chemical analyses, calculating the charge balance, the mineralization based on the major ions (Ca^{2+} , Mg^{2+} , Na^+ , K^+ , Cl^- ,

Table 1 Hydrogeochemistry of the groundwater samples for Turkana County

Sampling point	Coordinates		Year	pH	EC [mS/cm]	Na ⁺ [mg/L]	K ⁺ [mg/L]	Ca ²⁺ [mg/L]	Mg ²⁺ [mg/L]	Cl ⁻ [mg/L]	SO ₄ ²⁻ [mg/L]	HCO ₃ ⁻ [mg/L]	F ⁻ [mg/L]	NO ₂ ⁻ [mg/L]	NO ₃ ⁻ [mg/L]	Charge balance error [%]	Hydrochemical type ¹	
	X	Y																
1	35°34'42.4"E	3°06'45.9"N	2009	8.63	1.158	238.5	0.2	3.2	12.6	95.0	20.0	502.6	3.50	0.131	3.54	-0.02	Na-HCO ₃ -Cl	
2	35°37'41.80"E	2°21'47.30"N	2011	8.23	0.929	27.4	1.0	40.8	72.4	5.0	20.3	524.6	0.76	0.003	6.64	-0.54	Mg-Ca-HCO ₃	
3	35°39'06.40"E	2°22'40.05"N	2012	8.45	0.745	140.0	1.2	10.4	9.7	6.0	3.7	419.7	1.17	0.003	15.45	0.01	Na-HCO ₃	
4	35°30'12.07"E	1°56'47.14"N	2006	7.1	0.490	83.9	2.8	16.2	19.8	18.3	12.6	427.0	1.60	—	—	-12.15	Na-Mg-HCO ₃	
5	35°26'09.00"E	3° 02'38.00"N	2004	7.5	1.200	205.0	57.0	45.0	19.0	116.0	64.0	469.7	4.60	0.200	—	6.10	Na-HCO ₃ -Cl	
6	35°26'33.03"E	2°59'59.66"N	2009	8.26	0.945	153.5	1.4	24.0	18.5	116.0	50.0	297.7	1.00	0.763	10.62	0.05	Na-HCO ₃ -Cl	
7	36° 55'00"E	2°27'32.20"N	2014	8.1	0.509	84.0	3.0	16.0	19.3	14.0	11.0	366.0	1.20	—	—	-4.45	Na-Mg-HCO ₃	
8	36° 44'44.50"E	2°27'26.10"N	2015	7.4	1.208	92.0	5.0	18.0	23.0	16.0	12.0	329.4	0.80	—	—	5.95	Na-Mg-HCO ₃	
9	35°29'50.30"E	2°58'54.50"N	2012	8.15	1.843	378.0	6.7	12.0	14.6	138.0	0.4	878.4	1.31	0.003	5.84	-0.14	Na-HCO ₃ -Cl	
10	35°29'50.30"E	2°57'51.20"N	2008	7.96	2.680	464.8	5.6	48.0	48.6	100.0	287.5	1000.4	4.80	0.88	79.68	-0.02	Na-HCO ₃ -SO ₄	
11	36° 1'58.00"E	2°22'51.00"N	2005	7.5	1.900	421.6	19.0	10.0	6.2	200.0	80.0	756.4	0.50	—	—	0.26	Na-HCO ₃ -Cl	
12	36° 6'9.39"E	1°10'59.00"N	2006	7.4	0.765	114.9	22.8	135.0	55.6	33.0	57.6	378.2	1.89	—	—	33.42	Na-Ca-Mg-HCO ₃	
13	35°27'15.10"E	2°45'9.30"N	2011	8.03	3.630	583.0	2.0	56.0	97.2	220.0	783.0	805.2	2.10	—	31.87	-0.25	Na-Mg-SO ₄ -HCO ₃	
14	35°30'16.40"E	2°28'29.20"N	2014	7.8	0.755	90.0	4.2	18.0	20.0	16.0	14.0	359.9	1.20	—	—	-1.06	Na-Mg-HCO ₃	
15	35°32'56.00"E	2°12'56.00"N	2006	7	0.320	135.8	362.0	51.0	13.0	32.0	14.0	420.9	4.10	—	—	38.65	K-Na-HCO ₃	
16	35°23'1.92"E	3°13'49.74"N	2009	7.2	47.000	8364.0	7.6	656.0	880.0	15670.0	591.0	244.0	0.42	0.296	371.85	0.51	Na-Cl	
17	36°15'19.10"E	2°36'44.70"N	2010	8.09	0.281	23.1	3.1	20.3	4.9	5.0	1.0	148.8	0.15	0.011	1.30	-2.65	Na-Ca-Mg-HCO ₃	
18	35°38'35.78"E	2°45'17.72"N	2006	7.7	0.600	135.0	5.3	6.1	2.6	56.0	48.1	219.6	0.20	—	—	2.45	Na-HCO ₃	
19	35°39'21.00"E	2°36'40.00"N	2005	7.2	1.600	219.8	21.0	8.2	6.0	42.0	24.0	500.2	2.00	—	0.10	4.81	Na-HCO ₃	
20	35°24'45.06"E	4°46'49.38"N	2007	7.84	0.482	73.0	2.8	25.6	3.9	112.0	<0.3	97.6	0.73	—	0.14	0.47	Na-Ca-Cl-HCO ₃	
21	35°32'58.00"E	3° 6'19.00"N	2005	7.7	0.600	133.8	5.6	6.0	2.4	56.0	48.0	219.6	0.20	—	—	1.98	Na-HCO ₃ -Cl	
22	35°35'54.10"E	2°36'8.50"N	2012	8.06	0.815	159.0	0.6	8.8	9.2	8.0	4.3	463.6	1.28	0.003	10.31	-0.11	Na-HCO ₃	
23	35°38'44.60"E	2°21'58.90"N	2014	7.9	2.010	220.0	21.0	8.2	6.1	45.0	26.0	488.0	1.10	—	—	5.50	Na-HCO ₃	
24	35°22'35.00"E	3° 43'2.00"N	2009	8.34	3.350	765.0	1.8	0.8	2.0	750.0	117.0	556.3	1.70	0.10	27.45	0.41	Na-Cl-HCO ₃	
25	35°38'11.00"E	2°42'27.00"N	2006	7.7	0.600	133.8	5.6	6.0	2.4	56.0	48.0	219.6	0.20	—	—	1.98	Na-HCO ₃ -Cl	
26	35°29'48.00"E	3° 8'52.00"N	2005	8	3.800	8863.0	30.0	48.0	52.0	740.0	280.0	11468.0	0.80	0.800	15.00	9.94	Na-HCO ₃	
27	35°34'48.94"E	3° 6'50.40"N	2004	7.5	0.750	113.7	25.0	135.0	54.0	33.0	58.0	372.1	1.85	—	—	33.58	Ca-Na-Mg-HCO ₃	
28	35°25'48.88"E	2° 31'11.15"N	2006	7.1	0.490	85.0	3.2	16.1	18.9	12.0	9.2	359.9	1.50	—	—	-2.94	Na-HCO ₃ -Cl	
29	35°27'39.00"E	3° 29' 00"N	2005	7.6	0.890	171.7	6.4	14.0	6.0	100.0	64.0	292.8	0.40	—	—	-0.85	Na-HCO ₃ -Cl	
30	35°23'22.45"E	3° 7'26.38"N	2009	7.98	6.500	1456.0	3.0	8.0	14.6	1550.0	386.0	739.3	0.70	0.131	30.99	0.45	Na-Cl	
31	35°33'32.170"E	3° 7'30.50"N	2012	8.44	2.010	442.0	3.2	8.0	4.9	180.0	28.0	851.6	5.87	—	5.98	0.20	Na-HCO ₃ -Cl	
32	35°38'15.60"E	3° 6'12.70"N	2012	8.32	3.100	667.0	7.6	16.0	12.2	400.0	65.6	1071.2	2.21	0.03	33.33	0.23	Na-HCO ₃ -Cl	
33	36° 0'46.40"E	2°21'58.50"N	2016	8.2	1.037	170.0	6.0	12.0	5.1	95.0	55.0	280.6	n.a.	—	—	0.83	Na-HCO ₃ -Cl	
34	35°37'16.30"E	2°35'18.50"N	2011	7.71	0.871	99.5	10.5	29.6	31.6	20.0	11.4	466.0	0.70	0.003	14.87	-0.26	Na-Mg-HCO ₃	
35	35° 31'29.50"E	2°47'3.20"N	2012	8.43	0.870	97.8	10.4	31.0	31.6	16.0	11.4	463.6	0.64	0.003	24.30	-0.29	Na-Mg-HCO ₃	
WHO guideline value (2017)²																		
Kenyan potable water standard (2014)³																		
				5.5–9.5	2.500	200	—	150	100	250	400	—	—	1.5	0.003	45	—	—

¹Hydrochemical type of groundwater

²Exceeded values for the WHO guideline value are in bold

³Exceeded values for the Kenyan potable water standard are marked in red

* Not of health concern at levels found in drinking water (taste threshold are recommended, see WHO (2017)).

HCO_3^- and SO_4^{2-}) and denomination of the hydrochemical type of water.

The charge balance error was calculated for 35 points. For almost all samples charge balance error was acceptable (in range of $\pm 10\%$) except few ones (No. 4, 12, 15, and 27) possibly affected by the analytical methods used, physical parameters interfering with the measurements, and sampling method applied (Mika et al. 2018; Wątor et al. 2018, 2019; Rusiniak et al. 2020). Despite this, these samples were included in the statistical analysis and speciation modelling—a source of errors generated during sampling and laboratory instrumentation could not be verified based on the documentation and shortened chemical analysis reports gathered. Calculated mineralisation of the groundwater collected varies from 206.2 to 26,413 mg/L. The mineralization (M) is mainly controlled by the concentration of bicarbonates and sodium ions—there is a strong Pearson correlation between M and HCO_3^- ($R = 0.994$) and Na^+ ($R = 0.998$). Furthermore, there was observed a clear effect of Cl^- and SO_4^{2-} concentrations on the groundwater mineralization ($R = 0.714$ and $R = 0.372$, respectively). From these calculations, two sample outliers (saline water) which affected the calculations of correlation coefficient were excluded (No. 16 and 30). The analysed all water samples can be classified in a range from fresh, brackish to saline water based on mineralization parameter. As the Piper Diagram shows, groundwater types in Turkana County (Fig. 2) are mainly Na + K- HCO_3 , Ca-Mg- HCO_3 , Na + K-Cl, or Na- SO_4 .

4.1.2 Quality of the Turkana County groundwater from viewpoint of human consumption

To assess the suitability of groundwater collected across Turkana County for drinking purposes, current guidelines and legal regulations were used. The guidelines for drinking water quality published by the World Health Organization (2017) were adopted as the main reference. Additionally, the Kenyan Potable water standard (2014) was used in this assessment.

Among the chemical parameters included in this study, the guideline of WHO specify the maximum allowable concentration values only for fluoride, nitrite, and nitrate. The values specified for these indices are justified by proven real or potentially toxic effects on human health (WHO 2017). In the Kenyan Potable water standards and the EU regulations, there are already established maximum permissible levels for the following physicochemical parameters: magnesium, sodium, chlorides, sulphates, pH value, electrical conductivity, and also for calcium in the case of Kenyan regulations (Table 1).

Within the analysed parameters, groundwater samples from 17 wells met the requirements established in the

guideline and regulations mentioned with the simultaneous absence of data for nitrite and nitrate concentration in 10 samples (NO_2^-) and 9 samples (NO_3^-). The concentration of the fluoride was in the range of 0.15–5.87 mg/L. In 12 samples the concentration of F^- exceeded the WHO guideline value and the maximum permissible level contained in the Kenyan legislation of 1.5 mg/L. In 22 samples where the F^- concentration was below or equal to 1.5 mg/L, the calculated mean and median concentration is 0.77 and 0.75 mg/L, respectively. For higher concentrations the statistical parameters are 3.02 mg/L (mean) and 2.16 mg/L (median). Considering the results for the whole region, the mean concentration of 1.56 mg/L exceeds the guideline value of 1.5 mg/L, while the median suggests that the water is suitable for drinking purposes (1.19 mg/L). For the Nayane Katan sample, the fluoride concentration was not available.

The regional distribution of the fluoride ion showed no dependence on the borehole depth like in the publication of Abdurahman and Zewdie (2018). Only when the data is divided into subgroups based on the water-bearing formations (sediments, basement, and volcanic rocks), fluoride tend to show a negative correlation with depth in sedimentary rocks (Table 2). For basement and volcanic rocks, there was not found a significant correlation between F^- concentration and the borehole depth.

The fluoride constitutes the main problem in analysed groundwater due to its fairly high concentrations. Concentrations are often much higher than the guideline value led to skeletal fluorosis which is a problem met in Turkana County (Fig. 3).

Analysing subsequent parameters and it can be stated that the groundwater from the Turkana County did not meet the Kenyan potable water standard requirements for electrical conductivity (EC) (7 samples), sodium (14 samples), calcium (1 sample), magnesium (1 sample), chloride (5 samples) and sulphate concentrations (2 samples). Nitrite concentrations did not fulfil the regulations for groundwater collected from 10 wells, as well as the nitrate concentrations, exceeded the WHO guideline value and KPWS maximum permissible levels in 2 cases. The presence of nitrogen species in the groundwater seems to be rather linked to anthropogenic and not to geogenic sources and can be caused by cattle breeding and insufficient latrine isolation. Especially relatively high concentration of NO_3^- found under oxidizing conditions may be a result of water recharge with anthropogenic contaminants.

4.2 Speciation calculations

The hydrogeochemical modelling based on thermodynamic calculations is a common method for evaluation of water–rock interactions and water treatment processes (Appelo

Table 2 The correlation coefficient between F^- and depth in aquifer formations

Formation	Fluoride [mg/L] versus depth [m b.s.l.]	
	Pearson correlation coefficient	Significant at α value
All formations	– 0.219	0.22
Sedimentary rocks	– 0.621*	0.013
Basement	0.21	0.471
Volcanic rocks	0.625	0.375

*Correlation is significant at the 0.05 level (2-tailed)

**Fig. 3** Dental fluorosis in a child (photog. Piotr Stopa)

and Postma 2005; Tomaszewska et al. 2018) The results of chemical analyses were used for the calculation of speciation. Hydrogeochemical modelling was performed with PHREEQC 3.5 software (Parkhurst and Appelo 1999). Input data for initial solutions were pH, temperature, redox conditions (pe/ion pares), Na^+ , K^+ , Ca^{2+} , Mg^{2+} , HCO_3^- , SO_4^{2-} , Cl^- , NO_2^- , NO_3^- , F^- . To evaluate the chemical equilibrium state between solid phases and aqueous solution the saturation indices were calculated for each mineral phase of interest (Parkhurst and Appelo 1999). Because chemical analyses and determination of temperature adjusted equilibrium constants K_T are more or less biased with some error there is a widely adopted rule that the thermodynamic equilibrium between solution and concerned minerals phase is reached when the SI value is in the range of $\pm 5\%$ $\lg K_T$ (Dobrzyński 2006; Tomaszewska et al. 2017; Sekuła et al. 2020).

The redox conditions play an important role in the formation of the chemical composition of groundwater (Appelo and Postma 2005; Dobrzyński et al. 2018; Wątor et al. 2020). Thus, due to the lack of information about redox potential value (E_H), the nitrogen species were used to determine the redox conditions by the calculation of electron activity (pe) using the N(V)/N(III) redox couple. The groundwater samples exhibit very similar redox conditions—pe values are in the range of 7.16–8.27. In the case

of the lack of data for NO_2^- and NO_3^- concentrations, the pe value for the rest of the samples was calculated as a mean from the pe values computed for available redox species (NO_3^-/NO_2^-) due to the normal distribution of this parameter.

Saturation indices (SI) were calculated and plotted for selected minerals such as fluorite (CaF_2), anhydrite ($CaSO_4$), gypsum ($CaSO_4 \cdot 2H_2O$), and calcite ($CaCO_3$). Groundwater collected from all wells was undersaturated concerning anhydrite and gypsum despite a relatively high concentration of sulphate in several samples (Figs. 4, 5).

All samples showed very similar saturation indices for both phases. Groundwater undersaturated concerning sulphate minerals is capable to dissolve these phases assuming they are present in the rock matrix. Consequently, there can be precipitation of carbonates due to the common ion effect. It can be a reason for the relatively low concentration of HCO_3^- in samples with high SO_4^{2-} (Karegi et al. 2018).

Undersaturation with respect to calcite (Fig. 6) is found in 11 samples with the simultaneous low concentration of calcium (mean concentration of calcium for these points is 11.54 mg/L, medium 10.0 mg/L, minimum 0.8, and maximum 25.60 mg/L). The concentration of bicarbonates was 361.7 mg/L with a minimum value of 97.6 and a maximum of 756.4 mg/L. Under equilibrium state, there are 17 samples where the concentration of Ca was in the range from 3.2 to 656 mg/L, mean value of 70.1 mg/L, and median 18.0 mg/L. Also, the mean bicarbonate concentration is 429.2 mg/L, with a minimum of 148.8 mg/L and a maximum of 878.4 mg/L. There are 7 samples supersaturated concerning calcite and they are characterised by significantly higher concentrations of bicarbonate (mean value of 2312 mg/L, medium 851.6 mg/L, minimum 463.6 mg/L, and maximum value of 11468 mg/L).

The principal mineral of interest is fluorite and 6 samples are at equilibrium with this phase. The mean concentration of fluoride ion for these samples is relatively high and equals 3.85 mg/L, median 4.35 mg/L. The minimum value of 1.85 mg/L exceeded the WHO and Kenyan maximum permissible level for drinking water. The maximum value is almost 4 times higher than the recommended

Fig. 4 Saturation index for CaSO₄ legend: blue point—undersaturated solution number and names of sampling points consistently to Table 1

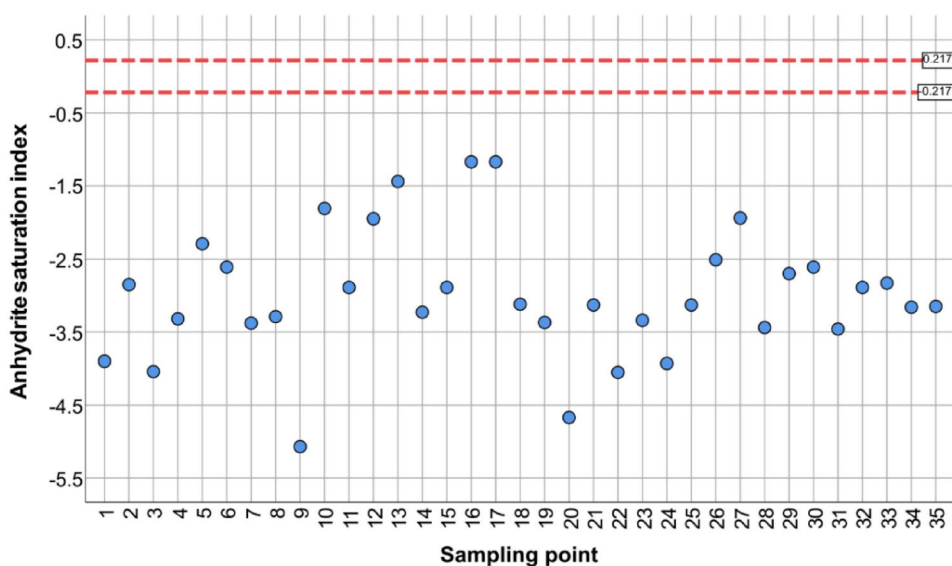
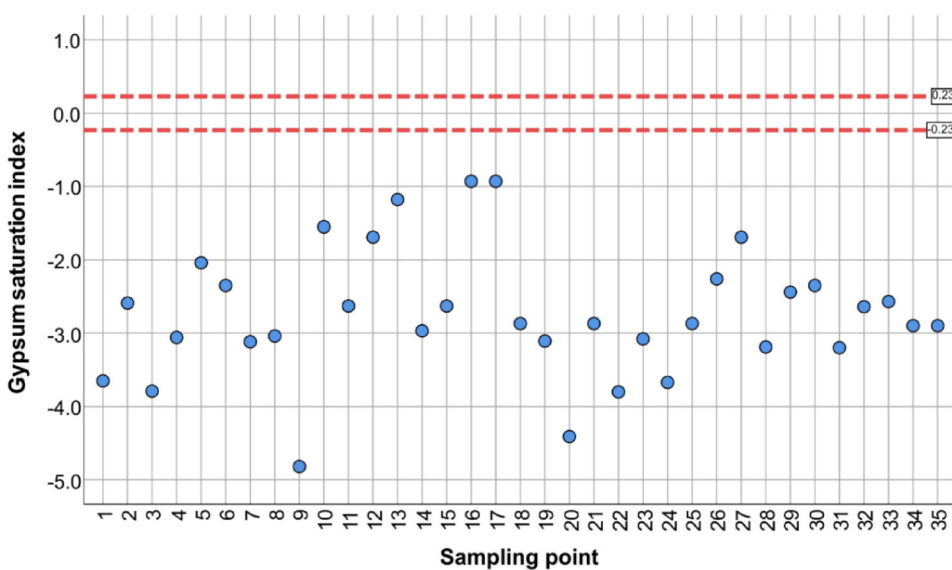


Fig. 5 Saturation index for CaSO₄·2H₂O legend: blue point—undersaturated solution



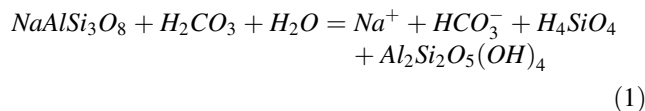
MPL, reaching 5.87 mg/L. The rest of the samples is undersaturated, and they can be enriched in fluoride ions (Fig. 7).

5 Discussion

5.1 Sources of high Na⁺ in groundwater

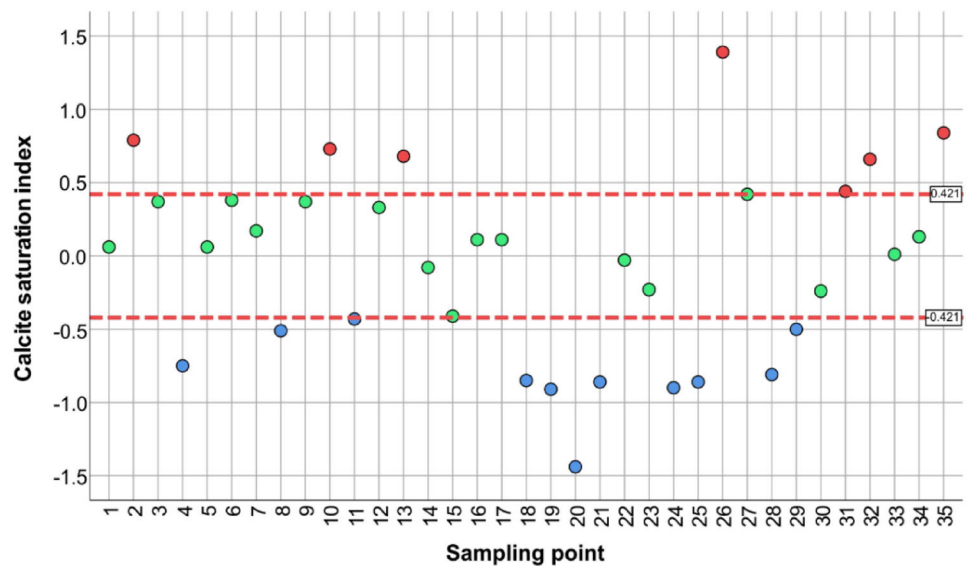
Most of the groundwater samples collected throughout Turkana County in Kenya are of the Na-HCO₃ hydrochemical type. Beyond Na⁺ as a dominant cation and HCO₃⁻ as an anion, in several samples there are other prevailing ions (> 20 % meq/L) such as Cl⁻ (16 samples), Mg²⁺ (10 samples), Ca²⁺ (4 samples), SO₄²⁻ (2 samples), and K⁺ (1 sample). In one sample (No. 27) there are no

dominant cations. The Na-HCO₃ type of water is less common compared to Ca-HCO₃ or Ca-Mg-HCO₃ types characteristic for freshwaters and resulting from the dissolution of the carbonate minerals such as calcite, aragonite, and dolomite. The process controlling the relatively high concentration of sodium in groundwater is chemical weathering of Na-feldspar (1) with the simultaneous release of sodium ions and bicarbonates (Toran and Saunders 1999; Dupalová et al. 2012; Kumar et al. 2017):

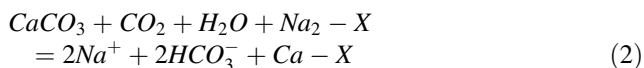


The production of Na⁺ and HCO₃⁻ in groundwater may also be caused by cation exchange of Na⁺ on exchange

Fig. 6 Saturation index for CaCO_3 legend: red point—supersaturated solution, green—thermodynamic equilibrium, blue—undersaturated solution



sites by Ca^{2+} coupled with dissolution of carbonates (Sracek and Hirata 2002; Sracek et al. 2019):



where X denotes exchange sites. Both processes produce Na- HCO_3 type of groundwater with high pH values and mineralization.

5.2 Fluoride ions sources in groundwater

In groundwater, the occurrence of fluoride is often linked to the volcanic rocks and its concentration is controlled by alkalinity, the concentration of bicarbonates, and electrical conductivity (Ali et al. 2016, 2018; Alarcón-Herrera 2013; Alarcón-Herrera et al. 2020; Saxena and Ahmed 2001). Groundwater enrichment in fluoride ions may have an origin in chemical weathering, magmatic processes, atmospheric dust, and industrial pollution. Precipitation of mineral-like CaCO_3 in solution with the slightly alkaline or alkaline pH value will favour decreasing of Ca ions concentration with simultaneous enrichment in F^- ions through the dissolution of fluorite until the thermodynamic equilibrium with this phase is reached (Gizaw 1996; Kumar and Singh 2015; Rafique et al. 2015). Groundwater around the world containing a high concentration of fluoride exhibits often the Na- HCO_3 type with a low concentration of calcium and/or magnesium ions (Alarcón-Herrera 2013; Sracek et al. 2015). Also, fluoride is present in groundwater as anion F^- and is desorbed at high pH values above pH_{ZPC} just like other anionic species of As, Mo, Se, and V (Appelo and Postma 2005). The link of high F^- to Na- HCO_3 type of groundwater has been observed, e.g., at the Chaco-Pampean Plain in Argentina (Smedley

et al. 2002; Bhattacharya et al. 2006), the Main Ethiopian Rift (Bretzler et al. 2011), and southeast and central Sri Lanka (Edmunds and Smedley 2004) with similar climatic and hydrogeological conditions as in the Turkana Lake region.

5.3 Correlation between F^- and Ca^{2+} ions

In research studies presented, e.g., by Gizaw (1996), Rafique et al. (2015), and Kumar et al. (2017) there was found an inverse relationship between the concentration of F^- and Ca^{2+} in investigated natural waters. It is related to the solubility control by precipitation fluorite when supersaturation concerning the mineral phase is reached. In the saturation indices plot, only 6 samples stay in thermodynamic equilibrium with CaF_2 (Fig. 8). For these points, there was a check of the equilibrium state with CaCO_3 . Two points, i.e., Kalemngorok (No. 10), and Nataparkakonok (No. 31) show supersaturation with this mineral phase manifesting a tendency for precipitation of calcite. Kapendo (No. 12) and Nakwamekwi parish BH (No. 27) samples are in the upper range of SI values and the Keenenyuk sample (No. 15) is in the middle of the interval for thermodynamic equilibrium. When these points are plotted, there is a significant Pearson correlation coefficient ($p < 0.05$) for the inverse correlation between calcium ions and fluoride ions with the value of $R = -0.993$ (Fig. 7a) as expected based on CaF_2 solubility control of dissolved F^- (Appelo and Postma 2005). However, when all points are included in the plot, there is no correlation (Fig. 7b), suggesting these processes operate only locally.

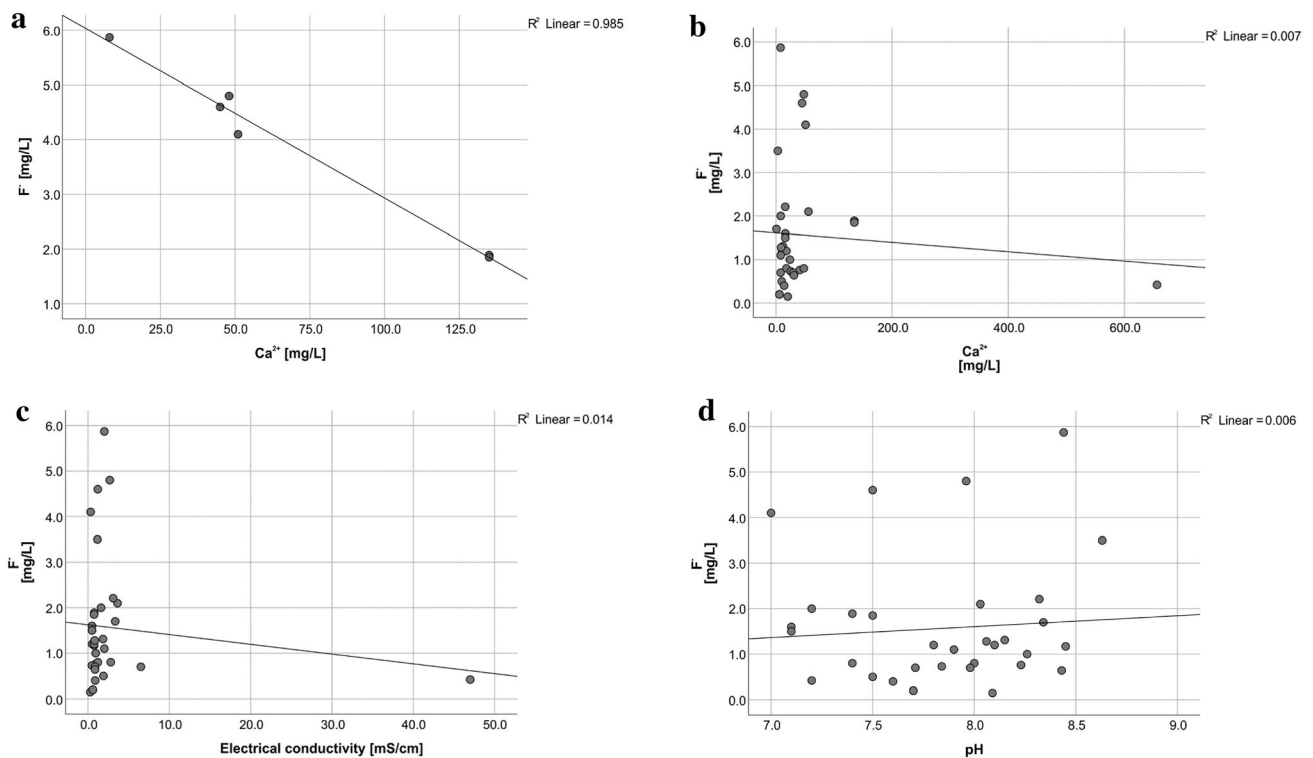
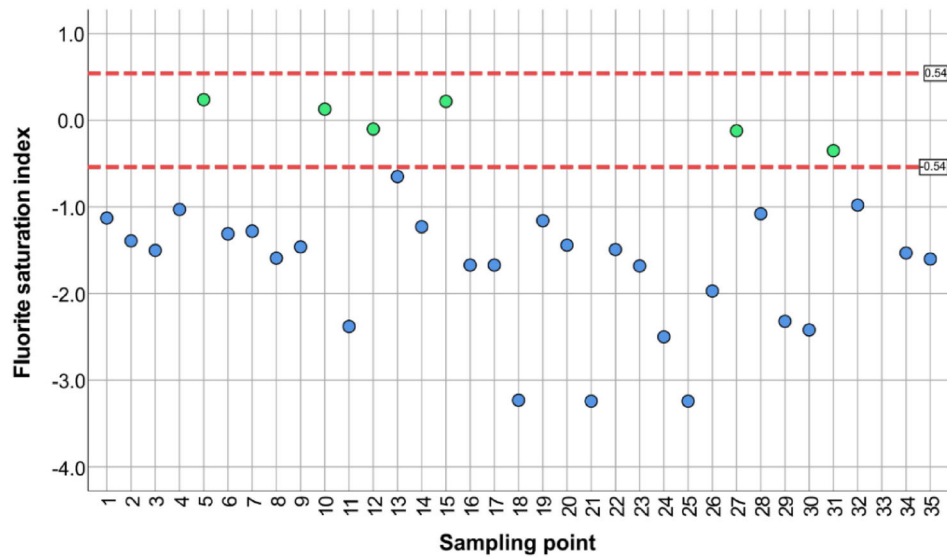


Fig. 7 Saturation index for CaF_2 legend: greent—hermodynamic equilibrium, blue—undersaturated solution

5.4 Correlation between F^- and EC, pH

There is no correlation between F^- and EC representing mineralization (Fig. 7c), suggesting that evaporation is not the principal process responsible for high F^- concentrations.

Similarly, the lack of correlation between pH and F^- (Fig. 7d), suggesting that desorption of F^- under increasing pH conditions is not significant. However, the possibility of competition with trace elements forming anionic species for adsorption sites should be checked in future studies.

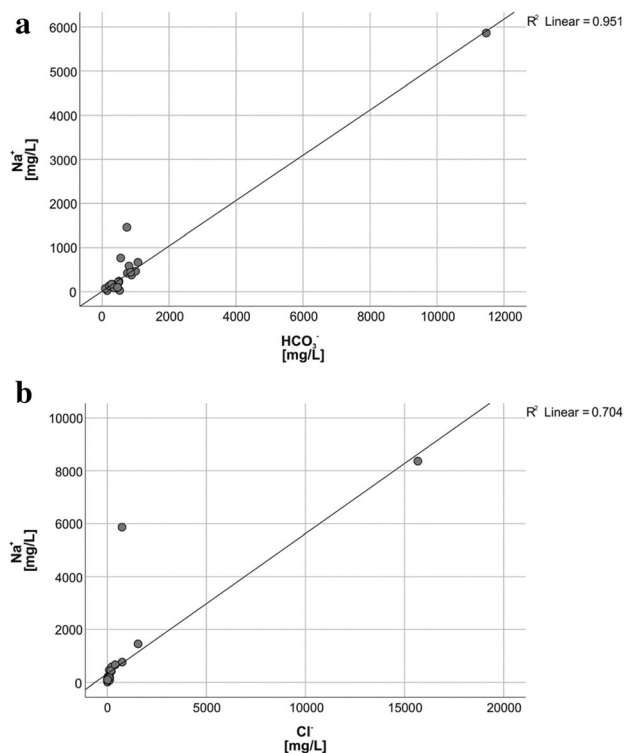


Fig. 8 a Na vs HCO_3^- for all data b Na vs Cl for all data

5.5 Relationship between Na^+ and F^- ions

Also, Na^+ ions have a strong positive correlation with HCO_3^- probably as a consequence of the sodium feldspar weathering in the aquifers and/or cation exchange coupled to the dissolution of carbonates (Fig. 8a). This correlation has been observed in F-rich groundwaters in Ethiopia (Bretzler et al. 2011) and Namibia (Sracek et al. 2015). For samples, where the sampled wells are installed in sandy riverbed sediments, a high concentration of sodium may be a result of hydraulic contact of groundwater with local surface water bodies. The water in the Kenyan rivers and lakes exhibit slightly alkaline to alkaline pH with increasing concentration of Na^+ , HCO_3^- , and Cl^- ions as a result of strong evaporation (Gizaw 1996; Cerling 1979; Yuretich and Cerling 1983). Concentrations of Na^+ and Cl^- increase in parallel (Fig. 8b) because both ions behave conservatively, i.e., they remain dissolved, until advanced evaporation stages with resulting formation of a brine (Drever 1997).

In our study concentration of sodium perhaps is mostly restricted to the water horizon which constitutes of sands and gravels with locally alternated with clay formation, weathered and/or fractured gneisses (granitoid, pegmatic, biotite, epidotised), and mafic rocks like basalts with

different degree of weathering and linked to the Tertiary volcanic rocks.

On a regional scale, F^- ions revealed only a slightly positive correlation ($R = 0.350$) with K^+ ions. It suggests that a potential source of F^- and K^+ in groundwater can be the dissolution of biotite (Chae et al. 2006), being one of the principal minerals in gneiss or weathered/fractured granitoid gneiss.

6 Conclusions

Investigations of the groundwater collected from the wells in the Turkana County in Kenya revealed relatively high concentrations of fluoride ions in the range from 0.15 to 5.87 mg/L. Almost half of the samples have a higher value of F^- than the WHO guideline value and the Kenyan potable water standard of 1.5 mg/L. Drinking water with an elevated concentration of fluoride can lead to health-related issues like dental or skeletal fluorosis or even to hypocalcaemia while precipitating CaF_2 in the human organism. Some prevention programs and water treatment should be applied to prevent negative (even serious) health problems that may result from the consumption of contaminated groundwater. Hydrogeochemical facies has shown that the groundwater in the majority is of Na- HCO_3 type which is significantly linked to high F^- concentrations, just like observed elsewhere, e.g., in Argentina, Ethiopia, and Namibia. These results suggest geogenic sources of F^- . Process of controlling the high concentration of F^- ions in groundwater seems to be precipitation of CaCO_3 decreasing Ca^{2+} concentration followed by the dissolution of CaF_2 and enrichment of groundwater in F^- . Simultaneously, chemical weathering of sodium feldspar in the aquifer matrix and cation exchange of Ca^{2+} for Na^+ on the exchange sites result in the formation of alkaline pH, Na- HCO_3 type of groundwater with a high concentration of F^- . Further studies should be focused on other trace elements forming anionic species like As and V.

Acknowledgements The authors are very thankful to the Government Chemist's Department of the Republic of Kenya and local institutions for sharing the data used in this paper.

Authors' contributions Conceptualization, P.R., K.S.; methodology, P.R.; formal analysis, P.R., O.S., K.S.; investigation, P.S., K.S., P.R.; writing—original draft preparation, P.R.; writing—review and editing, P.R., O.S., and K.S.; supervision, O.S. and K.S. All authors have read and agreed to the published version of the manuscript.

Funding The study was partially financed by AGH-UST 16.16.140.315/10.

Declarations

Conflict of interest The authors declare that they have no known competing financial interests or personal relationships that could have appeared to influence the work reported in this paper.

Open Access This article is licensed under a Creative Commons Attribution 4.0 International License, which permits use, sharing, adaptation, distribution and reproduction in any medium or format, as long as you give appropriate credit to the original author(s) and the source, provide a link to the Creative Commons licence, and indicate if changes were made. The images or other third party material in this article are included in the article's Creative Commons licence, unless indicated otherwise in a credit line to the material. If material is not included in the article's Creative Commons licence and your intended use is not permitted by statutory regulation or exceeds the permitted use, you will need to obtain permission directly from the copyright holder. To view a copy of this licence, visit <http://creativecommons.org/licenses/by/4.0/>.

References

- Abdurahman SG, Zewdie M (2018) Fluoride ion and total dissolved solid distribution in Ethiopian Rift valley: the case of Hawassa city aquifer. *J Hydrol Reg Stud* 19:240–249. <https://doi.org/10.1016/j.ejrh.2018.09.003>
- Abiye T, Bybee G, Leshomo J (2018) Fluoride concentrations in the arid Namaqualand and the Waterberg groundwater South Africa: understanding the controls of mobilization through hydrogeochemical and environmental isotopic approaches. *Ground Sustain Dev* 6:112–120. <https://doi.org/10.1016/j.gsd.2017.12.004>
- Alarcón-Herrera MT, Bundschuh J, Nath B, Nicolli HB, Gutierrez M, Reyes-Gomez VM, Nuñez D, Martín-Domínguez IR, Sracek O (2013) Co-occurrence of arsenic and fluoride in groundwater of semi-arid regions in Latin America: genesis, mobility and remediation. *J Hazard Mater* 262:960–969. <https://doi.org/10.1016/j.jhazmat.2012.08.005>
- Alarcón-Herrera MT, Martín-Alarcón DA, Gutiérrez M, Reynoso-Cuevas L, Martín-Domínguez A, Olmos-Márquez MA, Bundschuh J (2020) Co-occurrence possible origin and health-risk assessment of arsenic and fluoride in drinking water sources in Mexico: geographical data visualization. *Sci Total Environ* 698:134168. <https://doi.org/10.1016/j.scitotenv.2019.134168>
- Ali S, Thakur SK, Sarkar A, Shekhar S (2016) Worldwide contamination of water by fluoride. *Environ Chem Lett* 14(3):291–315. <https://doi.org/10.1007/s10311-016-0563-5>
- Ali S, Shekhar S, Bhattacharya P, Verma G, Chandrasekhar T, Chandrashekar AK (2018) Elevated fluoride in groundwater of Siwani Block Western Haryana India: a potential concern for sustainable water supplies for drinking and irrigation. *Ground Sustain Dev* 7:410–420. <https://doi.org/10.1016/j.gsd.2018.05.008>
- Ali S, Fakhri Y, Golbini M, Thakur SK, Alinejad A, Parseh I, Shekhar S, Bhattacharya P (2019a) Concentration of fluoride in groundwater of India: a systematic review meta-analysis and risk assessment. *Ground Sustain Dev*. <https://doi.org/10.1016/j.gsd.2019.100224>
- Ali W, Aslam MW, Junaid M, Ali K, Guo Y, Rasool A, Zhang H (2019b) Elucidating various geochemical mechanisms drive fluoride contamination in unconfined aquifers along the major rivers in Sindh and Punjab Pakistan. *Environ Pollut* 249:535–549. <https://doi.org/10.1016/j.envpol.2019.03.043>
- Apambire WB, Boyle DR, Michel FA (1997) Geochemistry, genesis, and health implications of fluoriferous groundwater in the upper regions of Ghana. *Environ Geol* 33(1):13–24. <https://doi.org/10.1007/s002540050221>
- Appelo CAJ, Postma D (2005) *Geochemistry groundwater and pollution*, 2nd edn. Balkema, Rotterdam
- Berger T, Mathurin FA, Drake H, Åström ME (2016a) Fluoride abundance and controls in fresh groundwater in Quaternary deposits and bedrock fractures in an area with fluorine-rich granitoid rocks. *Sci Total Environ* 569:948–960. <https://doi.org/10.1016/j.scitotenv.2016.06.002>
- Berger T, Yu C, Drake H, Peltola P, Svensson D, Åström ME (2016b) Fluorine geochemistry of quaternary deposits in a nemo-boreal catchment with elevated dissolved fluoride in surface waters and groundwater. *J Geochem Explor* 170:148–156. <https://doi.org/10.1016/j.gexplo.2016.09.003>
- Bhattacharya P, Claesson M, Bundschuh J, Sracek O, Fagerberg J, Jacks G, Martin RA, del Stornio A, Thir JM (2006) Distribution and mobility of arsenic in the Rio Dulce alluvial aquifers in Santiago del Estero Province, Argentina. *Sci Total Environ* 358(1–3):97–120. <https://doi.org/10.1016/j.scitotenv.2005.04.048>
- Bretzler A, Osenbrück K, Gloaguen R, Ruprecht JS, Kebede S, Stadler S (2011) Groundwater origin and flow dynamics in active rift systems - A multi-isotope approach in the Main Ethiopian Rift. *J Hydrol* 402(3–4):274–289. <https://doi.org/10.1016/j.jhydrol.2011.03.022>
- Cerling TE (1979) Paleochemistry of plio-pleistocene lake Turkana, Kenya. *Palaeogeogr Palaeoclimatol Palaeoecol* 27:247–285. [https://doi.org/10.1016/0031-0182\(79\)90105-6](https://doi.org/10.1016/0031-0182(79)90105-6)
- Chae GT, Yun ST, Kwon MJ, Kim YS, Mayer B (2006) Batch dissolution of granite and biotite in water: implication for fluorine geochemistry in groundwater. *Geochem J* 40(1):95–102. <https://doi.org/10.2343/geochemj.40.95>
- Chae GT, Yun ST, Mayer B, Kim KH, Kim SY, Kwon JS, Kim K, Koh YK (2007) Fluorine geochemistry in bedrock groundwater of South Korea. *Sci Total Environ* 385(1–3):272–283. <https://doi.org/10.1016/j.scitotenv.2007.06.038>
- Chief Geologist Mines and Geological Department (1962) *National Atlas of Kenya, Geological Map*, Survey of Kenya, Nairobi.
- Colombani N, Di Giuseppe D, Kebede S, Mastrocicco M (2018) Assessment of the anthropogenic fluoride export in Addis Ababa urban environment (Ethiopia). *J Geochem Explor* 190:390–399. <https://doi.org/10.1016/j.gexplo.2018.04.008>
- Craig L, Thomas JM, Lutz A, Decker DL (2018) Determining the optimum locations for pumping low-fluoride groundwater to distribute to communities in a fluoridic area in the Upper East Region Ghana. *Chem Geol* 476:481–492. <https://doi.org/10.1016/j.chemgeo.2017.12.001>
- Dehbandi R, Moore F, Keshavarzi B (2017) Provenance and geochemical behavior of fluorine in the soils of an endemic fluorosis belt central Iran. *J Afr Earth Sci* 129:56–71. <https://doi.org/10.1016/j.jafrearsci.2016.12.016>
- Dehbandi R, Moore F, Keshavarzi B (2018) Geochemical sources, hydrogeochemical behavior, and health risk assessment of fluoride in an endemic fluorosis area, central Iran. *Chemosphere* 19:763–776. <https://doi.org/10.1016/j.chemosphere.2017.11.021>
- Deng L, Zhang X, Zhang M, Jia X (2018) Effect of CaF₂ on viscosity structure and properties of CaO-Al₂O₃-MgO-SiO₂ slag glass ceramics. *J Non-Cryst Solids* 500:310–316. <https://doi.org/10.1016/j.jnoncrystol.2018.08.018>
- Dobrzyński D (2006) *Chemistry of groundwater*. In: Macioszczyk A (ed) *Basics of applied hydrogeology*. PWN, Warszawa
- Dobrzyński D, Kmiecik E, Wator K (2018) Oxidation reduction potential-an informative and unused indicator of curative and mineral water quality. *Acta Balneol* 60(4):233–238

- Dodson RG (1971) Geology of the Area South of Lodwar: Degree Sheet 18 NE Quarter with Coloured Geological Map (No 87). Republic of Kenya, Ministry of Natural Resources
- Drever JI (1997) The geochemistry of natural waters surface and groundwater environments, 3rd edn. Prentice Hall, Hoboken
- Dupalová T, Sracek O, Vencelides Z, Žák K (2012) The origin of thermal waters in the northeastern part of the Eger Rift, Czech Republic. *Appl Geochem* 27(3):689–702. <https://doi.org/10.1016/j.apgeochem.2011.11.016>
- Edmunds WM, Smedley PL (2004) Fluoride in natural waters. In: Selinus O (ed) *Essentials of medical geology*. Elsevier, Amsterdam
- Emenike CP, Tenebe IT, Jarvis P (2018) Fluoride contamination in groundwater sources in Southwestern Nigeria: assessment using multivariate statistical approach and human health risk. *Ecotox Environ Safe* 156:391–402. <https://doi.org/10.1016/j.ecoenv.2018.03.022>
- Enalou HB, Moore F, Keshavarzi B, Zarei M (2018) Source apportionment and health risk assessment of fluoride in water resources, south of Fars province, Iran: stable isotopes ($\delta^{18}\text{O}$ and δD) and geochemical modeling approaches. *Appl Geochem* 98:197–205. <https://doi.org/10.1016/j.apgeochem.2018.09.019>
- Ferrer N, Folch A, Lane M, Olago D, Odida J, Custodio E (2019) Groundwater hydrodynamics of an Eastern Africa coastal aquifer, including La Niña 2016–17 drought. *Sci Total Environ* 661:575–597. <https://doi.org/10.1016/j.envpol.2019.113646>
- Fordyce FM (2011) Fluorine: human health risks. In: Nriagu JO (ed) *Encyclopedia of environmental health*, vol 2. Elsevier, Amsterdam
- Fuge R (2019) Fluorine in the environment, a review of its sources and geochemistry. *Appl Geochem* 100:393–406. <https://doi.org/10.1016/j.apgeochem.2018.12.016>
- Gaciri SJ, Davies TC (1993) The occurrence and geochemistry of fluoride in some natural waters of Kenya. *J Hydrol* 143(3–4):395–412. [https://doi.org/10.1016/0022-1694\(93\)90201-J](https://doi.org/10.1016/0022-1694(93)90201-J)
- Gizaw B (1996) The origin of high bicarbonate and fluoride concentrations in waters of the Main Ethiopian Rift Valley, East African Rift system. *J Afr Earth Sci* 22(4):391–402. [https://doi.org/10.1016/0899-5362\(96\)00029-2](https://doi.org/10.1016/0899-5362(96)00029-2)
- Guo H, Zhang Y, Xing L, Jia Y (2012) Spatial variation in arsenic and fluoride concentrations of shallow groundwater from the town of Shahai in the Hetao basin, Inner Mongolia. *Appl Geochem* 27(11):2187–2196. <https://doi.org/10.1016/j.apgeochem.2012.01.016>
- Gupta R, Misra AK (2018) Groundwater quality analysis of quaternary aquifers in Jhajjar District Haryana India: focus on groundwater fluoride and health implications. *Alex Eng J* 57(1):375–381. <https://doi.org/10.1016/j.aej.2016.08.031>
- Handford CR (1987) Turkana Grits—a Cretaceous braided alluvial system in northern Kenya. *AAPG (Am Assoc Pet Geol) Bull; (United States)* 71(CONF-870606-)
- Hong X, Liang H, Chen Y, Liu Y, Shi Y (2018) Distribution of fluorine in the surface dust of Wuda coal base, Inner Mongolia of Northern China. *J Geochem Explor* 188:390–397. <https://doi.org/10.1016/j.gexplo.2018.02.012>
- Hsu CL, Lin WS, Lin CH, Liu J (2018) The effect of professional fluoride application program for preschool children in Taiwan: an analysis using the National Health Insurance Research Database (NHIRD). *J Dent Sci* 13(3):248–255. <https://doi.org/10.1016/j.jds.2018.04.001>
- Hu S, Luo T, Jing C (2013) Principal component analysis of fluoride geochemistry of groundwater in Shanxi and Inner Mongolia China. *J Geochem Explor* 135:124–129. <https://doi.org/10.1016/j.gexplo.2012.08.013>
- Kanagaraj G, Elango L (2019) Chromium and fluoride contamination in groundwater around leather tanning industries in southern India: implications from stable isotopic ratio $\delta^{53}\text{Cr}/\delta^{52}\text{Cr}$, geochemical and geostatistical modelling. *Chemosphere* 220:943–953. <https://doi.org/10.1016/j.chemosphere.2018.12.105>
- Karegi S, Macharia K, Muthengia W, Mwititi MJ (2018) Hydrogeochemistry of ground water in mbeere south sub-county, Kenya. *Int J Chem* 10(4):173–183. <https://doi.org/10.5539/ijc.v10n4p173>
- Khairnar MR, Dodamani AS, Jadhav HC, Naik RG, Deshmukh MA (2015) Mitigation of fluorosis—a review. *JCDR* 9(6):ZE05–ZE09
- Kravchenko J, Rango T, Akushevich I, Atlaw B, McCormick PG, Merola RB, Paul C, Weinthal E, Harrison C, Vengosh A, Jeuland M (2014) The effect of non-fluoride factors on risk of dental fluorosis: evidence from rural populations of the Main Ethiopian Rift. *Sci Total Environ* 488:595–606. <https://doi.org/10.1016/j.scitotenv.2013.12.087>
- Kumar A, Singh CK (2015) Characterization of hydrogeochemical processes and fluoride enrichment in groundwater of south-western Punjab. *Water Qual Expo Health* 7(3):373–387
- Kumar P, Singh CK, Saraswat C, Mishra B, Sharma T (2017) Evaluation of aqueous geochemistry of fluoride enriched groundwater: a case study of the Patan district, Gujarat, Western India. *Water Sci* 31(2):215–229. <https://doi.org/10.1016/j.wsj.2017.05.002>
- Kumar S, Venkatesh AS, Singh R, Udayabhanu G, Saha D (2018) Geochemical signatures and isotopic systematics constraining dynamics of fluoride contamination in groundwater across Jamui district, Indo-Gangetic alluvial plains, India. *Chemosphere* 205:493–505. <https://doi.org/10.1016/j.chemosphere.2018.04.116>
- KWPS (2014) Kenya Standard potable water specification KS EAS 12: 2014 ICS 1306020 First Edition.
- Laxmankumar D, Satyanarayana E, Dhakate R, Saxena PR (2019) Hydrogeochemical characteristics with respect to fluoride contamination in groundwater of Maheshwarm mandal, RR district, Telangana state, India. *Ground Sustain Dev* 8:474–483. <https://doi.org/10.1016/j.gsd.2019.01.008>
- Martins VTDS, Pino DS, Bertolo R, Hirata R, Babinski M, Pacheco DF, Rios AP (2018) Who to blame for groundwater fluoride anomaly in São Paulo Brazil? Hydrogeochemistry and isotopic evidence. *Appl Geochem* 90:25–38. <https://doi.org/10.1016/j.apgeochem.2017.12.020>
- Mika A, Waŋtor K, Kmiecik E (2018) Determination of fluorides in mineral and curative water—method validation. *Acta Balneol* 60(4):258–263
- Milojkovic DV, Silvestre OF, Stanić VD, Janjić GV, Mutavdžić DR, Milanović M, Nieder JB (2020) Fabrication and characterization of luminescent Pr³⁺ doped fluorapatite nanocrystals as bioimaging contrast agents. *J Lumin* 217:116757. <https://doi.org/10.1016/j.jlumin.2019.116757>
- Mondal D, Gupta S, Reddy DV, Nagabhushanam P (2014) Geochemical controls on fluoride concentrations in groundwater from alluvial aquifers of the Birbhum district, West Bengal, India. *J Geochem Explor* 145:190–206. <https://doi.org/10.1016/j.gexplo.2014.06.005>
- Msonda KWM, Masamba WRL, Fabiano E (2007) A study of fluoride groundwater occurrence in Nathenje, Lilongwe, Malawi. *Phys Chem Earth Pt A/b/c* 32(15–18):1178–1184. <https://doi.org/10.1016/j.pce.2007.07.050>
- Naderi M, Jahanshahi R, Dehbandi R (2020) Two distinct mechanisms of fluoride enrichment and associated health risk in springs' water near an inactive volcano, southeast Iran. *Ecotox Environ Safe* 195:110503. <https://doi.org/10.1016/j.ecoenv.2020.110503>

- Nair KR, Manji F, Gitonga JN (1984) The occurrence and distribution of fluoride in groundwaters of Kenya. *East Afr Med J* 61(7):503–512
- Ochungo EA, Ouma GO, Obiero JPO, Odero NA (2020) Impact of Drought on Ground Water Quality in Langata Sub-County, Kenya. *Am J Water Resour* 8(3):145–154. <https://doi.org/10.12691/ajwr-8-3-5>
- Oduor A, Cherogony K, Mutune J, Malesu M, Karuma A, Cherogony M, Nyolei D, Kandagor J, Onyango D (2012) Food security master plan for Turkana County. Diocese of Lodwar.
- Olaka LA, Wilke FD, Olago DO, Odada EO, Mulch A, Musolff A (2016) Groundwater fluoride enrichment in an active rift setting: central Kenya Rift case study. *Sci Total Environ* 545:641–653. <https://doi.org/10.1016/j.scitotenv.2015.11.161>
- Ozsvath DL (2006) Fluoride concentrations in a crystalline bedrock aquifer Marathon County, Wisconsin. *Environ Geol* 50:132–138. <https://doi.org/10.1007/s00254-006-0192-6>
- Parkhurst DL, Appelo CAJ (1999) User's guide to PHREEQC—a computer program for speciation reaction-path 1D-transport and inverse geochemical calculations. US Geol Survey Water-Resour Investig Rep 99:4259
- Pauwels H, Négrel P, Dewandel B, Perrin J, Mascré C, Roy S, Ahmed S (2015) Hydrochemical borehole logs characterizing fluoride contamination in a crystalline aquifer (Maheshwaram India). *J Hydrol* 525:302–312. <https://doi.org/10.1016/j.jhydrol.2015.03.017>
- Pettifor JM, Schnitzler CM, Ross FP, Moodley GP (1989) Endemic skeletal fluorosis in children: hypocalcemia and the presence of renal resistance to parathyroid hormone. *Bone Miner* 7(3):275–288. [https://doi.org/10.1016/0169-6009\(89\)90084-6](https://doi.org/10.1016/0169-6009(89)90084-6)
- Podder S, Akbari S, Roy S (2012) Cryolite induced morphological change in the compound eye of *Drosophila melanogaster*. *Fluoride* 45(1):58–64
- Rafique T, Naseem S, Ozsvath D, Hussain R, Bhangar MI, Usmani TH (2015) Geochemical controls of high fluoride groundwater in Umakot sub-district, Thar Desert, Pakistan. *Sci Total Environ* 530:271–278. <https://doi.org/10.1016/j.scitotenv.2015.05.038>
- Raj D, Shaji E (2017) Fluoride contamination in groundwater resources of Alleppey, southern India. *Geosci Front* 8(1):117–124. <https://doi.org/10.1016/j.gsf.2016.01.002>
- Raju NJ (2017) Prevalence of fluorosis in the fluoride enriched groundwater in semi-arid parts of eastern India: geochemistry and health implications. *Quat Int* 443:265–278. <https://doi.org/10.1016/j.quaint.2016.05.028>
- Rango T, Bianchini G, Beccaluva L, Tassinari R (2010) Geochemistry and water quality assessment of central Main Ethiopian Rift natural waters with emphasis on source and occurrence of fluoride and arsenic. *J Afr Earth Sci* 57(5):479–491. <https://doi.org/10.1016/j.jafrearsci.2009.12.005>
- Rango T, Kravchenko J, Atlaw B, McCornick PG, Jeuland M, Merola B, Vengosh A (2012) Groundwater quality and its health impact: an assessment of dental fluorosis in rural inhabitants of the Main Ethiopian Rift. *Environ Int* 43:37–47. <https://doi.org/10.1016/j.envint.2012.03.002>
- Rango T, Vengosh A, Jeuland M, Tekle-Haimanot R, Weinthal E, Kravchenko J, McCornick P (2014) Fluoride exposure from groundwater as reflected by urinary fluoride and children's dental fluorosis in the Main Ethiopian Rift Valley. *Sci Total Environ* 496:188–197. <https://doi.org/10.1016/j.scitotenv.2014.07.048>
- Rango T, Vengosh A, Jeuland M, Whitford GM, Tekle-Haimanot R (2017) Biomarkers of chronic fluoride exposure in groundwater in a highly exposed population. *Sci Total Environ* 596:1–11. <https://doi.org/10.1016/j.scitotenv.2017.04.021>
- Rashid A, Guan DX, Farooqi A, Khan S, Zahir S, Jehan S, Khattak SA, Khan MS, Khan R (2018) Fluoride prevalence in groundwater around a fluorite mining area in the flood plain of the River Swat, Pakistan. *Sci Total Environ* 635:203–215. <https://doi.org/10.1016/j.scitotenv.2018.04.064>
- Reddy DV, Nagabhushanam P, Sukhija BS, Reddy AGS, Smedley PL (2010) Fluoride dynamics in the granitic aquifer of the Wailapally watershed, Nalgonda District, India. *Chem Geol* 269(3–4):278–289. <https://doi.org/10.1016/j.chemgeo.2009.10.003>
- Rusiniak P, Ruzszczyńska A, Wątor K, Bulska E, Kmiecik E (2020) Methodological aspects concerning sampling and determination of total selenium and selenium species in geothermal waters. *Bull Geogr Phys Geogr Ser* 18(1):5–16. <https://doi.org/10.2478/bgeo-2020-0001>
- Saxena V, Ahmed S (2001) Dissolution of fluoride in groundwater: a water-rock interaction study. *Environ Geol* 40(9):1084–1087. <https://doi.org/10.1007/s002540100290>
- Sekula K, Rusiniak P, Wator K, Kmiecik E (2020) Hydrogeochemistry and related processes controlling the formation of the chemical composition of thermal water in Podhale Trough, Poland. *Energies* 13(21):5584
- Singh G, Kumari B, Sinam G, Kumar N, Mallick S (2018) Fluoride distribution and contamination in the water, soil and plants continuum and its remedial technologies, an Indian perspective—a review. *Environ Pollut* 239:95–108. <https://doi.org/10.1016/j.envpol.2018.04.002>
- Smedley PL, Nicolli HB, Macdonald DMJ, Barros AJ, Tullio JO (2002) Hydrogeochemistry of arsenic and other inorganic constituents in groundwaters from La Pampa, Argentina. *Appl Geochem* 17(3):259–284. [https://doi.org/10.1016/S0883-2927\(01\)00082-8](https://doi.org/10.1016/S0883-2927(01)00082-8)
- Sracek O, Hirata R (2002) Geochemical and stable isotopic evolution of the Guarani Aquifer System in the state of São, Paulo Brazil. *Hydrogeol J* 10(6):643–655. <https://doi.org/10.1007/s10040-002-0222-8>
- Sracek O, Wanke H, Ndakunda NN, Mihaljević M, Buzek F (2015) Geochemistry and fluoride levels of geothermal springs in Namibia. *J Geochem Explor* 148:96–104. <https://doi.org/10.1016/j.gexplo.2014.08.012>
- Sracek O, Geršl M, Faimon J, Bábek O (2019) The geochemistry and origin of fluids in the carbonate structure of the Hranice Karst with the world's deepest flooded cave of the Hranická Abyss, Czech Republic. *Appl Geochem* 100:203–212. <https://doi.org/10.1016/j.apgeochem.2018.11.013>
- Su H, Wang J, Liu J (2019) Geochemical factors controlling the occurrence of high-fluoride groundwater in the western region of the Ordos basin, northwestern China. *Environ Pollut* 252:1154–1162. <https://doi.org/10.1016/j.envpol.2019.06.046>
- Tekle-Haimanot R, Melaku Z, Kloos H, Reimann C, Fantaye W, Zerihun L, Bjorvatn K (2006) The geographic distribution of fluoride in surface and groundwater in Ethiopia with an emphasis on the Rift Valley. *Sci Total Environ* 367(1):182–190. <https://doi.org/10.1016/j.scitotenv.2005.11.003>
- Tiercelin JJ, Potdevin JL, Morley CK, Talbot MR, Bellon H, Rio A, Le Gall B, Vétel W (2004) Hydrocarbon potential of the Meso-Cenozoic Turkana Depression, northern Kenya. I. Reservoirs: depositional environments diagenetic characteristics, and source rock-reservoir relationships. *Mar Petrol Geol* 21(1):41–62. <https://doi.org/10.1016/j.marpetgeo.2003.11.007>
- Tomaszewska B, Rajca M, Kmiecik E, Bodzek M, Bujakowski W, Tyszer M, Wator K (2017) Process of geothermal water treatment by reverse osmosis. The research with antiscalants. *Desalin Water Treat* 73:1–10
- Tomaszewska B, Kmiecik E, Wątor K, Tyszer M (2018) Use of numerical modelling in the prediction of membrane scaling. Reaction between Antiscalants and Feedwater. *Desalination* 427:27–34. <https://doi.org/10.1016/j.desal.2017.11.004>

- Toran LE, Saunders JA (1999) Modeling alternative paths of chemical evolution of Na-HCO₃-type groundwater near Oak Ridge, Tennessee USA. *Hydrogeol J* 7(4):355–364. <https://doi.org/10.1007/s100400050208>
- Turkana Drilling Consortium (2008) Environmental Impact Assessment Project Report For Proposed Exploratory Oil And Natural Gas Well drilling Programme in Block 10BB: Turkana South and Turkana Central.
- Turkana Drilling Consortium (2010) Project Report for Environmental Impact Assessment of the Proposed Exploratory Well Drilling in Block 10BB: Turkana South and Turkana Central Districts by Africa Oil Kenya BV
- Ullah R, Zafar MS, Shahani N (2017) Potential fluoride toxicity from oral medicaments: a review. *Iran J Basic Med Sci* 20(8):841. <https://doi.org/10.22038/IJBMS.2017.9104>
- Walsh J, Dodson RG (1969) Geology of northern Turkana degree sheets 1 2 9 and 10 (No. 82). Geological Survey of Kenya
- Wang M, Li X, He WY, Li JX, Zhu YY, Liao YL, Yang JY, Yang XE (2019) Distribution, health risk assessment, and anthropogenic sources of fluoride in farmland soils in phosphate industrial area, southwest China. *Environ Pollut* 249:423–433. <https://doi.org/10.1016/j.envpol.2019.03.044>
- Wątor K, Kmiecik E, Rusiniak P (2018) An influence of research methodology on the results of determination of a chemical composition of curative water. *Acta Balneol* 60(4):272–276
- Wątor K, Kmiecik E, Postawa A, Rusiniak P (2019) A probabilistic approach to assessment of the quality of drinking water. *Geologos* 25(3):249–254
- Wątor K, Dobrzyński D, Sugimori K, Kmiecik E (2020) Redox potential research in the field of balneochemistry: case study on equilibrium approach to bioactive elements in therapeutic waters. *Int J Biometeorol*. <https://doi.org/10.1007/s00484-020-01871-7>
- WHO (2017) Guidelines for drinking-water quality: fourth edition incorporating the first addendum Geneva. World Health Organization; 2017 Licence: CC BY-NC-SA 3.0 IGO
- Wu C, Wu X, Qian C, Zhu G (2018) Hydrogeochemistry and groundwater quality assessment of high fluoride levels in the Yanchi endorheic region northwest China. *Appl Geochem* 98:404–417. <https://doi.org/10.1016/j.apgeochem.2018.10.016>
- Yadav KK, Kumar S, Pham QB, Gupta N, Rezaia S, Kamyab H, Yadav S, Vymazal J, Kumar V, Tri DQ, Talaiekhosani A, Prasad S, Reece LM, Singh N, Maurya PK, Cho J (2019a) Fluoride contamination, health problems and remediation methods in Asian groundwater: a comprehensive review. *Ecotox Environ Safe* 182:109362. <https://doi.org/10.1016/j.ecoenv.2019.06.045>
- Yadav KK, Kumar V, Gupta N, Kumar S, Rezaia S, Singh N (2019b) Human health risk assessment: study of a population exposed to fluoride through groundwater of Agra city, India. *Regul Toxicol Pharm* 106:68–80. <https://doi.org/10.1016/j.yrtph.2019.04.013>
- Yuretich RF, Cerling TE (1983) Hydrogeochemistry of Lake Turkana, Kenya: mass balance and mineral reactions in an alkaline lake. *Geochim Cosmochim Acta* 47(6):1099–1109. [https://doi.org/10.1016/0016-7037\(83\)90240-5](https://doi.org/10.1016/0016-7037(83)90240-5)
- Zango MS, Sunkari ED, Abu M, Lermi A (2019) Hydrogeochemical controls and human health risk assessment of groundwater fluoride and boron in the semi-arid northeastern region of Ghana. *J Geochem Explor* 207:106363. <https://doi.org/10.1016/j.gexplo.2019.106363>
- Zevenbergen C, Van Reeuwijk LP, Frapporti G, Louws RJ, Schuling RD (1996) A simple method for defluoridation of drinking water at village level by adsorption on Ando soil in Kenya. *Sci Total Environ* 188(2–3):225–232. [https://doi.org/10.1016/0048-9697\(96\)05174-1](https://doi.org/10.1016/0048-9697(96)05174-1)
- Zhang LE, Huang D, Yang J, Wei X, Qin J, Ou S, Zhang Z, Zou Y (2017) Probabilistic risk assessment of Chinese residents' exposure to fluoride in improved drinking water in endemic fluorosis areas. *Environ Pollut* 222:118–125. <https://doi.org/10.1016/j.envpol.2016.12.074>